applied sciences

MDPI

Article

A Long-Term Dynamic Analysis of Heat Pumps Coupled to Ground Heated by Solar Collectors

Vincenzo Ballerini, Eugenia Rossi di Schio, Paolo Valdiserri *, Claudia Naldi and Matteo Dongellini

Department of industrial Engineering DIN, Alma Mater Studiorum—University of Bologna, Viale Risorgimento 2, 40136 Bologna, Italy; vincenzo.ballerini2@unibo.it (V.B.); eugenia.rossidischio@unibo.it (E.R.d.S.); claudia.naldi2@unibo.it (C.N.); matteo.dongellini@unibo.it (M.D.)

* Correspondence: paolo.valdiserri@unibo.it; Tel.: +39-051-2093303

Abstract: In agreement with the decarbonization of the building sector to meet the 2050 climate neutrality targets, borehole thermal storage for solar energy represents a potential solution to increase the energy efficiency of renewable energy plants. As is well known, electricity is not the optimum solution to integrate large inflows of fluctuating renewable energy. In the present paper, we investigate the possibility to use the solar collector to give energy to the borehole field. In detail, a solar-assisted geothermal heat pump is applied to a school located in Milan, Italy. In winter, both the energy from the solar collector and the heat pump are collected into a storage tank connected to the emission terminals, whereas, in summer, as there is no energy demand, the hot water from the solar collector flows into the geothermal probes. By means of this seasonal thermal energy storage technology, the intermittent solar energy collected and stored during the summer months can be utilized during the winter months when the heating demand is high. A long-term dynamic analysis is performed by employing Trnsys. The results show that solar collectors coupled with ground-source heat pumps can give an important contribution to the soil temperature drift, and this also applies in cases of unbalanced loads during the heating season. Moreover, the employment of solar collectors increases the seasonal coefficient of performance of the heat pumps and may rise to reductions to the probes field.

Keywords: ground-source heat pumps; solar collectors; Trnsys; dynamic simulations

Citation: Ballerini, V.; Rossi di Schio, E.; Valdiserri, P.; Naldi, C.; Dongellini, M. A Long-Term Dynamic Analysis of Heat Pumps Coupled to Ground Heated by Solar Collectors. *Appl. Sci.* **2023**, *13*, 7651. https://doi.org/10.3390/app13137651

Academic Editor: Dimitris Mourtzis

Received: 19 May 2023
Revised: 19 June 2023
Accepted: 26 June 2023
Published: 28 June 2023

1. Introduction

In Europe, natural gas is widely used for winter heating, and, nowadays, many greenhouse gas emissions still come from burning fossil fuels [1]. For this reason, the European directives have obliged the European States to develop alternative renewable energy sources, such as solar, wind, and geothermal, to reduce the carbon dioxide emissions in the atmosphere [2,3]. Heat pumps and solar thermal systems realize the objective to reduce fossil fuels and to achieve decarbonization goals, including net zero greenhouse gas emissions at 2050 [4]. Heat pumps are particularly helpful for winter heating in temperate and mild climates and, therefore, could be particularly effective in Italy. A general analysis of the Italian energy system is reported in [5] and focuses on the possible energy, economic, and environmental effects of the use of individual heat pumps for winter space heating. Another aspect driving the decarbonization goals in the building sector is related to the envelope. For instance, different researchers investigated the use of glass facades [6–8].

Concerning the heat generation system, in the literature, many papers have investigated the evaluation of the seasonal coefficient of performance (SCOP) of heat pumps, both geothermal [9–12] and air-source, also considering, in the latter case, the effect of the defrosting cycle [13]. Regarding the integration of heat pumps with solar panels, the so-called solar-assisted heat pump systems, the most used system considers a heat pump connected to photovoltaic panels [14,15]. These systems suffer from a decrease

in electric conversion efficiency, mainly at the latitudes of Southern Europe, when the temperature in the solar collectors rises. Moreover, in [16], the authors demonstrate that climate changes have influenced PV energy production in the past period and will continue to cause a reduction in energy production.

In fewer papers, attention is paid to hybrid solar–geothermal heat pumps, although solar thermal panels and geothermal heat pumps have a high potential to reach the objective of the Paris Agreement [17]. As stated by Guelpa and Verda [18], thermal storage facilities ensure a heat reservoir for optimally tackling the dynamic characteristics of district heating systems. Ciampi et al. [19] simulated a solar district heating system for a period of 5 years when serving a district composed of six typical single-family houses under the climatic conditions of Naples (central Italy). The analysis showed that the use of a seasonal borehole TES connected to a solar DH system allowed for a primary energy reduction of 6% and a reduction in carbon dioxide emission of more than 4%. Another work [20] demonstrated that seasonal storage combined with a solar plant could decrease energy consumption by about 26%. An experimental study [21] of a ground-coupled heat pump used in a 180 m^2 private residence, combined with thermal solar collectors, showed that the energy injected into the ground was 34% of the heat extracted from the ground by using a heat pump with a COP of 3.75 after 11 months of operation. In a recent work [22], the authors investigated, by means of dynamic simulation over a 15-year period, a solar-assisted, ground-coupled heat pump system that met the domestic hot water demand of 960 students. The simulation outcomes regarding the underground heat balance were compared with a standalone heat pump. The results showed that solar energy storage in the ground could lessen the thermal imbalance caused by continuous heat extraction and correspondingly could improve the system's performance. In addition, when the entire system was employed in regions where solar energy resources were consistent, the average temperature of the soil may increase year by year instead of decreasing as when a stand-alone heat pump is used. Thermal energy storage presents many advantages with respect to other storage systems, when compared with batteries in particular. Lund et al. [23] criticized electricity storage because more efficient and cheaper options existed. They asserted that electricity was not the optimum solution to integrate large inflows of fluctuating renewable energy.

As already discussed, previous published papers asserted that electricity was not the optimum solution to integrate large inflows of fluctuating renewable energy. In the present work, the long-term behavior of a solar-assisted ground source heat pump was analyzed. The case study was represented by a school virtually located in Italy, in the city of Milan. In the summer periods, while there was no energy demand in the school, the solar collector gave energy to the borehole field. The novelty of the present analysis, in fact, consisted of using the solar collectors to restore the soil in order to increase the COP of the ground source heat pump or to reduce the probe's field. Different simulations were carried out varying the number of probes and the area of the solar collectors, in order to determine the soil temperature for 15 years, comparing the seasonal performances of the heat pump.

2. Materials and Methods

2.1. Building

The school under investigation is represented in Figure 1. It is a two-floor building ideally located in Milan, Italy (Coordinates: 45°27′39.24″ N 9°16′48″ E), i.e., with 2404-degree days and a heating period from 15 October to 14 April every year. In the building, below the ground floor, there is a non-heated basement. As reported in Table 1, the total floor area of the two floors is 2313 m^2 (total volume 8424 m^3); the gymnasium and the stairwell have a height of 6 m, whereas all the other thermal zones have a height of 3 m.

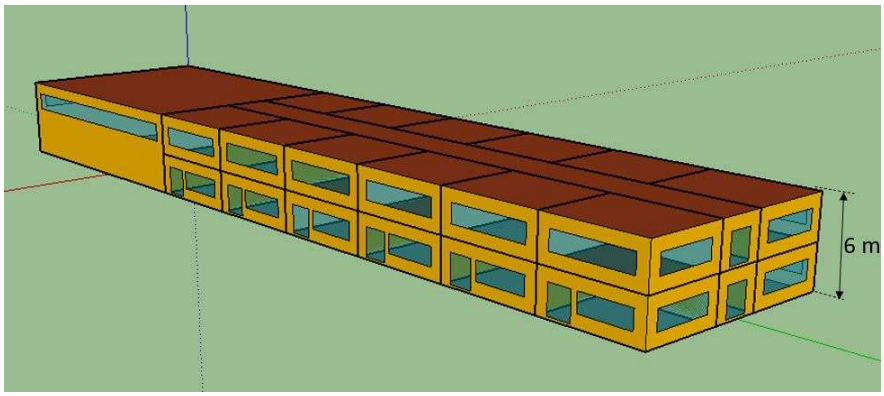

(**a**)

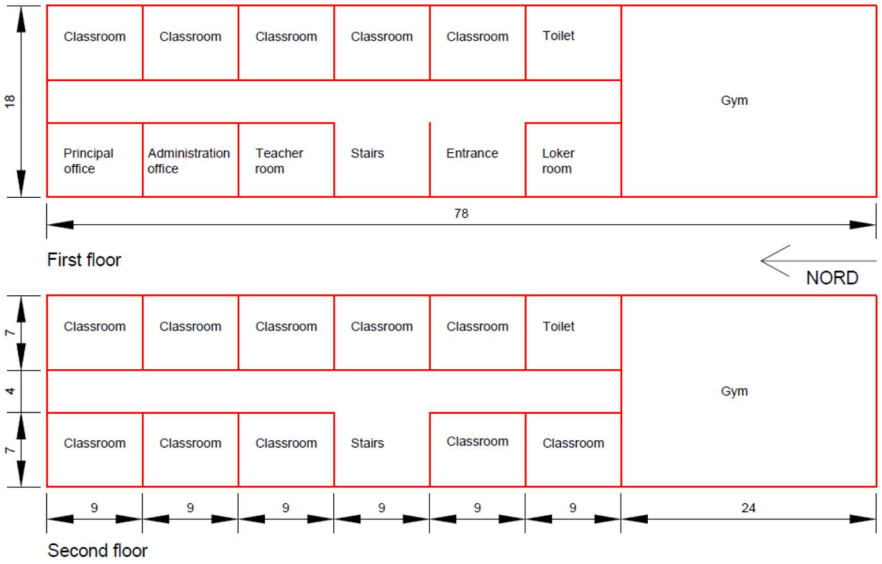

(**b**)

Figure 1. Three-dimensional view of the building under investigation (**a**) and school plan (**b**).

Table 1. Floor area (S_{floor}) of each zone.

Zone	S_{floor} (m^2)
Classrooms	945
Toilets	126
Secretariat	63
Presidency	63
Teachers' offices	63
Stairwell	63
Entrance	63
Gymnasium	432
Corridors	432
Locker room	63
Total	2313

In Table 2, the thermal transmittances of the main elements are reported. Concerning windows, they are double glazed (4/12/4 mm), having a low-emission treatment, they are argon-filled with a wooden frame, and display a total transmittance U = 1.69 W/(m^2K). Moreover, the external walls have an insulation thickness of 10 cm; thus, the building can be considered well insulated for the Milan climate.

Table 2. Thermal transmittance *U* of the main elements.

Element	U (W/(m^2·K)
External walls	0.292
Ceiling	0.287
Floor	0.342
Partitions	1.098
Windows	1.690

The set points are reported in Table 3 and were applied as valid for every day of the heating season from Monday to Saturday; on Sunday and during nighttime, we assumed that the heating was turned off. Public holidays were not considered.

Table 3. Set points.

Zone	$t_{set\text{-}point}$ (°C) (7:00–17:30)	$t_{set\text{-}point}$ (°C) (17:00–7:00)	S_{floor} (m^2)
Classrooms, toilets, secretariat, Presidency, teachers' offices	20	-	1260
Corridors, stairwell, entrance	18	-	558
Locker room	22	-	63
Gymnasium	18	-	432

2.2. Heating System

The heating system displayed fan coils as emission terminals, modeled in TRNSYS with a fan and a heating coil (type 744 and 753d, respectively). The temperature was controlled by zone, and the thermostat had 3 stages relating to fan speed (0.6/0.75/1 P_{max}).

The fan coils were sized according to an external design temperature of −5 °C and to reach the set-point temperature of 20 °C in about 1 h.

The air and water flow rates of the fan coils were estimated by relating them to the thermal power of the emission terminal, considering a commercial model (Daikin): 140 kg/(h kW) for water and 150 kg/(h kW) for air. Details of the fan coils for each heating zone are reported in Table 4, and the Trnsys sketch of the emission system is reported in Figure 2.

Table 4. Details of the fan coils for each heating zone.

Zone	Power (kW)	Water (kg/h)	Air (kg/h)
A1	4.5	630	675
A2	4.5	630	675
A3	4.5	630	675
A4	4.5	630	675
A5	4.5	630	675
B1	4.5	630	675
B2	4.5	630	675
B3	4.5	630	675
B4	4.5	630	675
B5	4.5	630	675
C1	4.5	630	675
C2	4.5	630	675
C3	4.5	630	675
C4	4.5	630	675
C5	4.5	630	675
gymnasium	44.0	4600	6600
locker room	5.0	700	750
toilet ground floor	4.5	630	675
toilet first floor	4.5	630	675
corridor ground floor	9.35	1000	1403
corridor first floor	10.5	1100	1575
entrance	3.0	300	450
stairwell	4.3	600	645
presidency	4.5	630	675
teachers' offices	4.5	630	675
secretariat	4.5	630	675

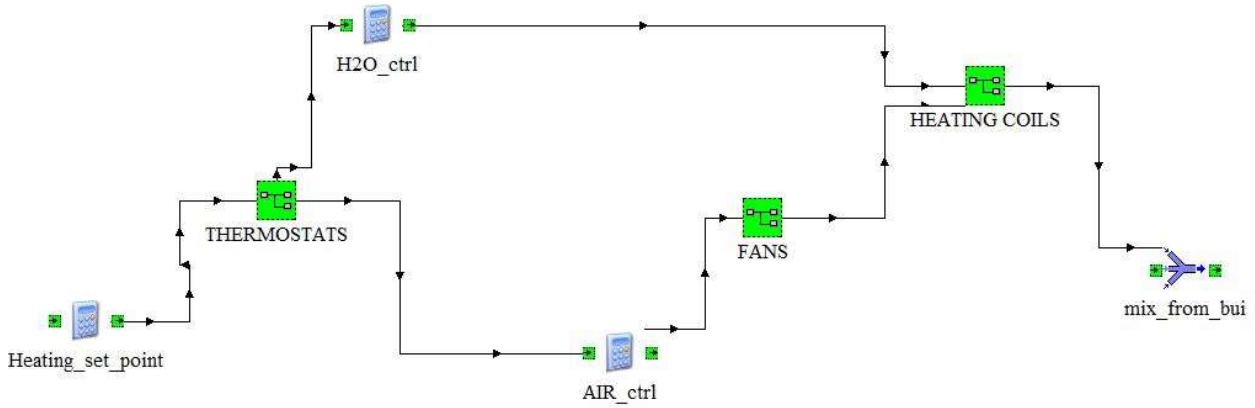

Figure 2. Sketch of the emission system, as built in Trnsys.

Regarding the generator system, it was assumed that two water-water heat pumps of 40 kW each could operate together or separately. The heat pumps were modelled with thermal power and COP maps for 3 different inverter frequency values, as shown in Figure 3.

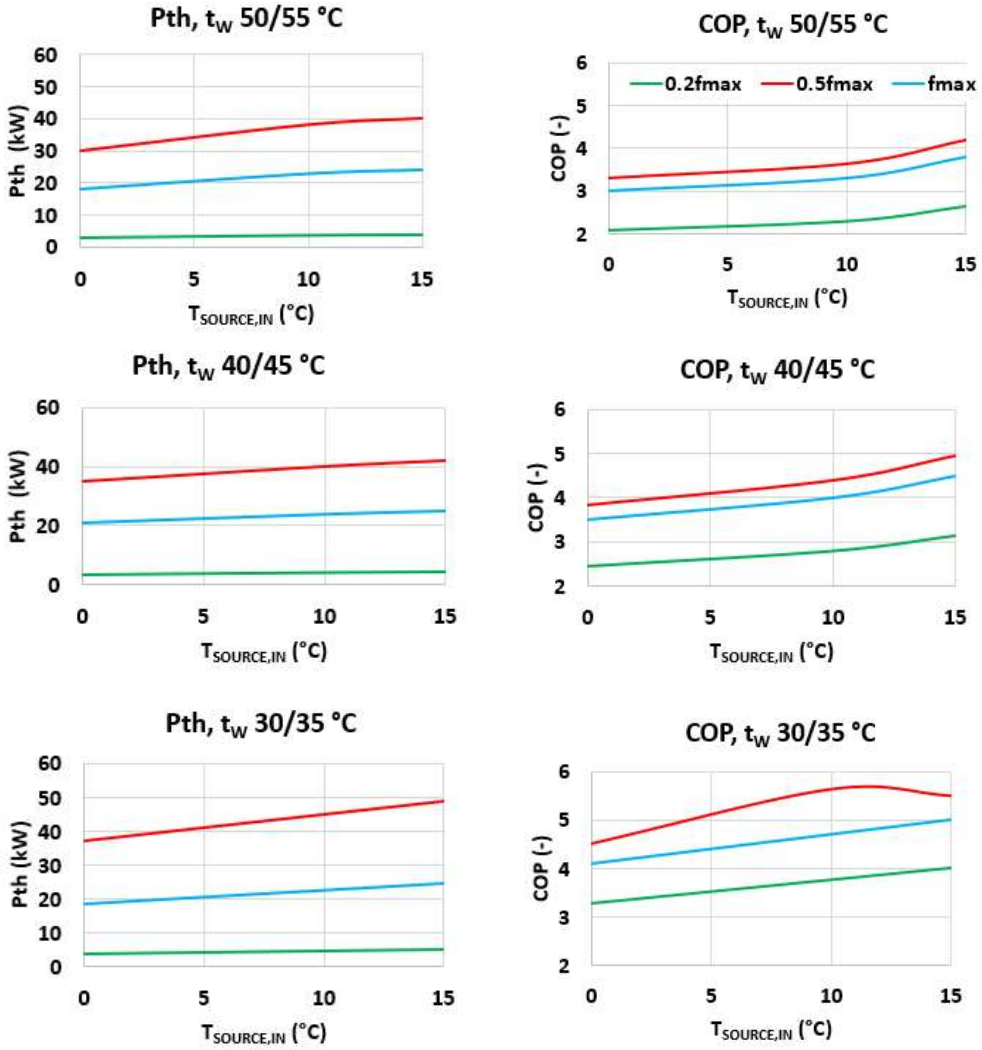

Figure 3. Thermal power P_{th} and *COP* of the heat pumps vs. water source temperature $T_{SOURCE,IN}$ for different inverter frequencies and for different water inlet and outlet temperatures.

The plant included a 2000 L storage tank (Type 156), i.e., 50 L/kW referred to the power of the generators. The storage tank was located in the basement of the building, and it had an internal coil (heat exchanger) dedicated to solar energy (internal and external diameter of the pipes equal to 0.020 m and 0.022 m, respectively; coil length 200 m, coil thermal conductivity 400 W/(mK)). The storage tank was also connected to the emission terminals (maximum flow rate of 22,000 kg/h) and to the heat pump (22,000 kg/h); regarding the solar collectors, a flow rate of 1500–3000 kg/h was set, depending on the simulation scenario considered. All pumps were variable speed (Type 110). Concerning the plant working conditions, the winter and summer conditions are sketched in Figure 4. In particular, in winter, the water from the solar collector flowed into the heat exchanger inside the storage tank; the heated water contained in the storage was moved to the emission terminals, which supplied hot air to the single rooms of the building. The heat pump ran and operated between two circuits (heat pumps–tank and heat pumps–borehole field circuit). In summer, no energy demand for cooling the building was assumed; therefore, the water from the solar collector flowed in the geothermal probes.

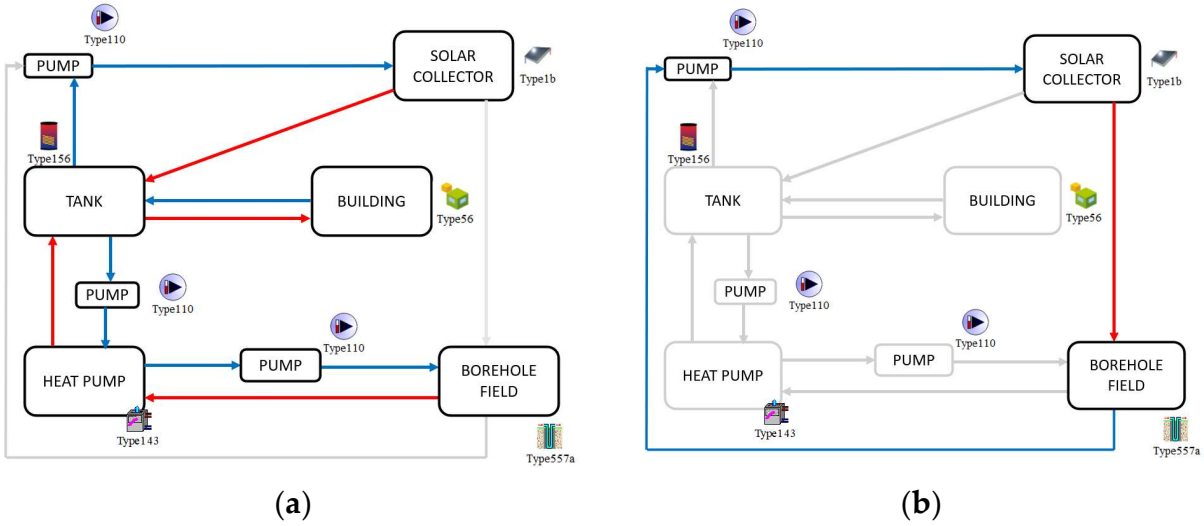

Figure 4. Plant working conditions in winter (**a**) and in summer (**b**); the grey lines represent non-active connections during the specific season.

To perform the Trnsys simulations [24,25], the following assumptions were made. The air changes were assumed to be equal to 0.5 h^{-1} when there were no people, whereas they were equal to 0.9 h^{-1} when the building was occupied (Mon–Sat from 7:00 to 17:30). Occupancy was 25 people in the classrooms and the gym; 2 in the toilets, offices, and locker room; and 5 in the corridors, teachers' offices, and secretariat. The sensible load for each person was considered equal to 60 W (40 W radiative and 20 W convective gain), whereas, for the latent part, the production of 0.065 kg/h of vapor per person was considered in all rooms except the gym, where a production of 0.45 kg/h per person was assumed. The solar control foresaw that the solar pump was activated for the outlet temperature from the collector higher than 10 K, with respect to the tank temperature in winter, whereas it foresaw activation during the summer only if the inlet temperature to the probes was higher than 10 K compared to the temperature of the water leaving the probe. The pump, in this case, had variable speed control.

2.3. Ground Probes and Solar Collectors

In order to numerically simulate the ground probes, for the soil a density of 2800 kg/m^3, a conductivity 1.8 W/(mK) and a thermal capacity 0.85 kJ/(kgK) were assumed. The probes were single U-tubes, having outer diameters of 0.2 m, pipe center distances of 0.1 m, pipe outer diameters of 33 mm; the depths of the probes were 100 m. The pipe conductivity was 0.4 W/(mK), whereas the sealing mortar conductivity was 1.6 W/(mK). An initial soil

temperature of 14 °C was estimated, and a Type 557a was used. The approximate sizing, according to the ASHRAE method, provided a probe field of 2.7 km if the presence of solar energy was neglected. In order to simulate the behavior of the solar collectors, Trnsys Type 1b was employed, considering values of the intercept efficiency of 0.807, efficiency slope of 3.766 W/(m^2·K), curvature efficiency of 0.0059 W/(m^2·K^2), and collector slope of 35° (south direction). The total surface area of the collectors was different for the groups of simulations, as reported in the next chapter.

3. Results and Discussion

Twelve different simulations were conducted, varying the number of probes and the areas of the solar collectors in order to determine the soil temperature for 15 years. Details of the simulations are reported in Table 5. Table 5 also reports the storage volumes of the soils considered for the simulations by Type 557a: for every simulation, a soil volume in order to neglect the boundary effects on the simulations and the soil temperature results has been assumed. The mass flow rate of the solar pump has been determined in order to obtain a flow rate of 50 L/m^2 for the installed collector.

Table 5. Simulations performed.

#	Number of Probes	Solar Panels (m^2)	Solar Pump (m^3/h)	Storage Volume (m^3)
A1	25	0	0	135,000
A2	20	0	0	108,000
A3	15	0	0	81,000
A4	10	0	0	54,000
A5	25	30	1.5	135,000
A6	20	30	1.5	108,000
A7	15	30	1.5	81,000
A8	10	30	1.5	54,000
A9	25	40	2	135,000
A10	20	40	2	108,000
A11	15	40	2	81,000
A12	10	40	2	54,000

In Table 6, the average annual thermal energies (averaged over the 15 years of simulations conducted) and the electricity demands related to the geothermal heat pumps are reported for each simulation.

Table 6. Annual thermal energy given by the heat pump to the storage (*ET*) and electricity consumption (*EE*) obtained from simulations. The values reported are the mean average during the 15 years of Trnsys simulations.

#	*EE* (MWh)	*ET* (MWh)
A1	12.37	46.35
A2	12.51	46.30
A3	12.68	46.24
A4	12.97	46.03
A5	11.26	43.10
A6	11.33	42.79
A7	11.56	43.00
A8	11.86	43.02
A9	10.98	42.32
A10	11.11	42.29
A11	11.28	42.22
A12	11.53	42.07

Cases A1–A4 are presented in Table 6 (i.e., with no solar collectors), and an increase in electricity demand of 5% for case A4 (total length of ground probes of 1 km) with respect to case A1 (total length of 2.5 km) can be noticed.

It can also be noticed that in the simulations from A1 to A4 the thermal energy given to the storage was higher compared to the subsequent simulations (an average of 46.23 MWh for simulations from A1 to A4, compared to the average of 42.65 MWh for simulations from A5 to A12).

In Table 7, the thermal energy required and injected in the borehole field are reported for each simulation, together with the thermal energy given by the solar collector (if included in the analysis) to the hot water tank during winter and the one supplied to the borehole field during the summer.

Table 7. Annual thermal energy taken from the borehole field ($ET_{BF,tot}$), sum of the thermal energy taken by the heat pump during winter season ($ET_{BF,winter}$), and thermal energy given to the ground by the solar collector during summer ($ET_{BF,summer}$). Yearly thermal energy given by the solar collectors ($ET_{SC,tot}$), sum of solar energy given during winter ($ET_{SC,winter}$) and summer ($ET_{SC,summer}$). The values reported are the mean average during the 15 years of Trnsys simulations.

#	$ET_{BF,tot}$ (MWh)	$ET_{BF,summer}$ (MWh)	$ET_{BF,winter}$ (MWh)	$ET_{SC,tot}$ (MWh)	$ET_{SC,winter}$ (MWh)	$ET_{SC,summer}$ (MWh)
A1	−33.99	0	−33.99	0	0	0
A2	−33.80	0	−33.8	0	0	0
A3	−33.55	0	−33.55	0	0	0
A4	−33.07	0	−33.07	0	0	0
A5	−10.16	21.69	−31.85	21.69	3.69	25.38
A6	−10.58	20.89	−31.47	20.89	3.99	24.88
A7	−9.78	21.66	−31.44	21.66	3.69	25.35
A8	−9.36	21.80	−31.16	21.80	3.49	25.29
A9	−2.60	28.75	−31.35	28.75	4.63	33.38
A10	−2.48	28.70	−31.18	28.70	4.63	33.33
A11	−2.33	28.61	−30.94	28.61	4.63	33.24
A12	−2.15	28.40	−30.55	28.40	4.64	33.04

If we focus on Table 7, we can see that the thermal energy taken from the ground is always higher than the energy given to it, as it is also in cases A9–A12 (cases considering a collector surface area of 40 m^2): the total energy unbalanced to the ground ranges between −33.99 MWh for case A1 to −2.15 MWh in case A12.

If we consider the data related to the thermal energy supplied by the solar collectors for the simulation groups with the same areas, namely, A5–A8 (30 m^2) and A9–A12 (40 m^2), we observe that there is a comparable increase in the thermal energy supplied by the collectors during the summer (31.7%) despite an increase in the collection area of approximately 33.3%. However, during the heating season, the increase is more modest (going from an average of 3.72 MWh in cases A5–A8 to a mean value of 4.63 in cases A9–A12, resulting in a percentage increase of 24.5%). The slight increase in solar collector production during winter by increasing the area does not appear to have significant effects on the thermal energy extracted from geothermal probes during winter, considering the two simulation groups (A5–A8 averaging 31.48 MWh and A9–A12 averaging 30.75 MWh). However, when considering the annual difference between the thermal energy extracted from the geothermal field during winter and the energy provided during the summer period for the same simulation group, the cases from A9 to A12 show an average annual thermal energy extraction of 2.39 MWh compared to 9.97 MWh for the A9–A12 group, representing a reduction of approximately 76% in energy extraction.

In Figures 5 and 6, the trends in the soil temperature around the borehole field and the *SCOP* for the 15 years of dynamic analysis are reported, respectively.

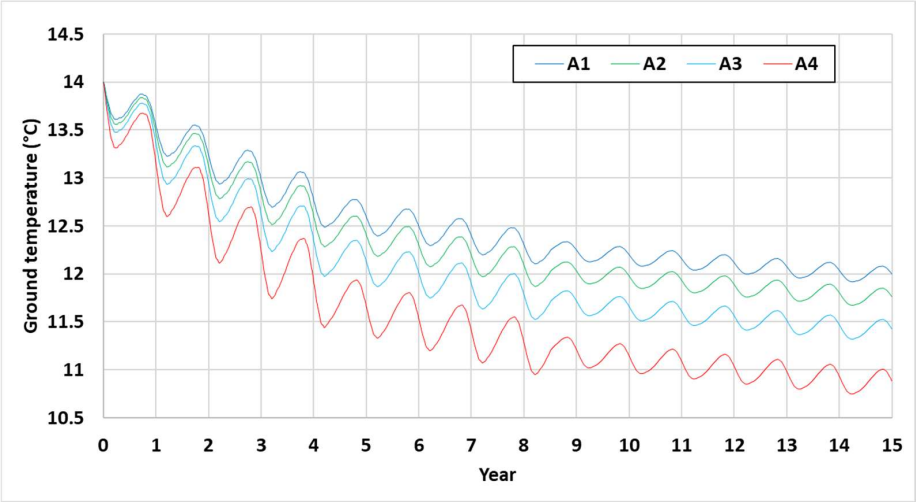

(**a**)

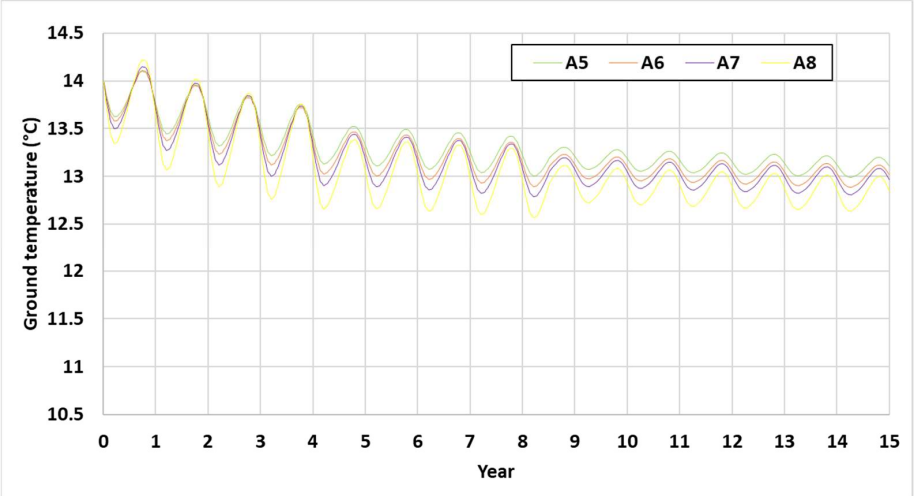

(**b**)

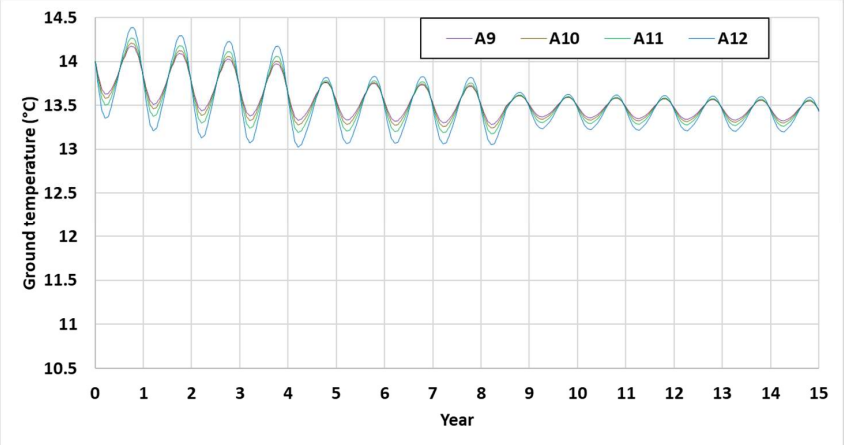

(**c**)

Figure 5. Trends in the ground temperature obtained from dynamic simulations for the different considered scenarios: A1 to A4 (**a**), A5 to A8 (**b**), A9 to A12 (**c**).

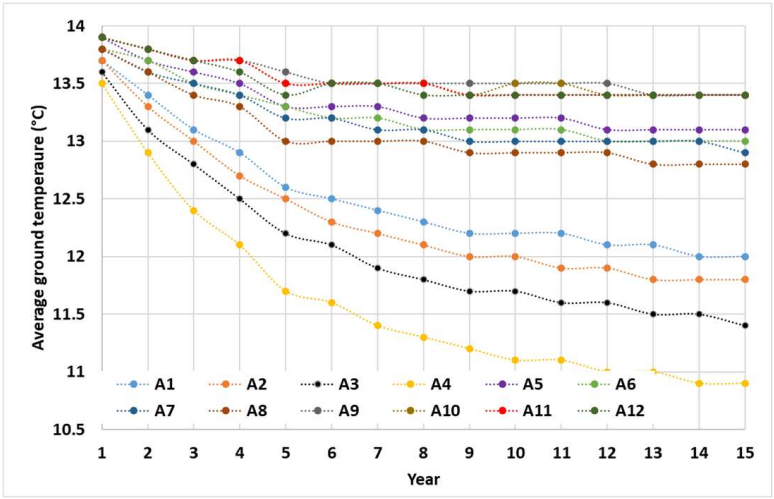

(**a**)

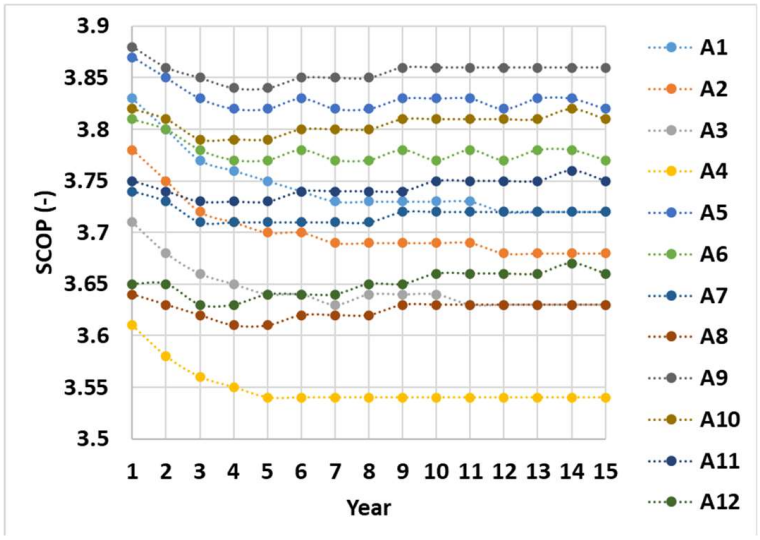

(**b**)

Figure 6. Yearly mean soil temperature (**a**) and *SCOP* of the water-to-water heat pump (**b**).

Regarding cases A1–A4, Figures 5 and 6 show a decrease in the ground temperature of the field and a decrease in the *SCOP* (ground temperature for cases A1 and A4 of 12 °C and 10.9 °C, respectively, at the fifteenth year of the dynamic simulation; *SCOP* in the last year of 3.72 and 3.54 for cases A1 and A4, respectively). A peculiar aspect regards the *SCOP* and ground temperature trends in case A4: the *SCOP* trends tend to be constant starting from the fifth year, whereas the ground temperature shows a decreasing trend also in the latter years of the simulations. Figure 5a shows no important changes in the amplitude of the ground temperature for cases A1–A4, even if the ground field is undersized.

The reduction in thermal energy demand from the ground field obtained using the solar collectors in cases A5–A12 leads to a stabilization of the ground temperature after five years at values between 12.8 °C and 13.4 °C (13.4 °C is obtained by the four simulations A9–A12 that consider a collector area of 40 m^2. The use of solar collectors leads to a stabilization of the *SCOP*, similar to cases A1–A4, but to higher values (Figure 6b)).

In all the cases that consider the solar collectors with respect to cases A1–A4, from Figure 5b,c, an increase in ground temperature amplitude during the year can be observed: in particular, the amplitude results higher for the cases that present undersized probes (i.e., A8, A7, A11, and A12) with respect to the well-sized ground field.

Furthermore, Figure 5 shows that the amplitude of temperature fluctuations tends to decrease as the number of simulation years increases, compared to the early simulation years, stabilizing and being consistently higher in the case of the undersized borehole field systems compared to the well-sized borehole field systems, even in the presence of solar thermal panels. Meanwhile, the *SCOP* tends to stabilize in the final years of the simulation.

Another aspect that can be observed from Figure 6 is the increase in *SCOP* considering the same ground field due to the coupling with solar collectors: for instance, if we consider that the field was made of 25 boreholes, the case without solar collectors (case A1) and the case in which the field was coupled with solar collectors (cases A5 and A9), the percentage increases in the *SCOP* in the fifteenth year were 2.7% and 3.8%, respectively, for A5 and A9l, with respect to A4. When analyzing the *SCOP* for the undersized field made of 10 boreholes, the increases were 2.5% and 3.7%, respectively, for A8 and A12, with respect to A4.

4. Conclusions

In the present paper, a numerical analysis of ground-coupled heat pumps coupled with solar collectors is presented. The main findings of this work are:

- The solar collectors coupled with ground-source heat pumps can make an important contribution to soil temperature drift, and this also adds to cases of unbalanced loads during the heating season;
- The influence of the solar collectors can be observed also on the *SCOP* values during the years: in particular, the SCOP tends to be higher in cases that employ the solar collectors;
- The *SCOP* obtained in the last year of simulation, in the case that considers 40 m^2 of solar collectors instead of 30 m^2, is slightly higher, but the influence of the solar collector dimension has a limited impact on the *SCOP* itself (case A9, with respect to case A5, shows an increase on *SCOP* of 1%). However, considering the cases characterized by the same collector area, as in, for example, cases A9–A12, the SCOP decrease due to the undersized ground field is up to 5% by the fifteenth year of the dynamic simulations.

Despite the reduction in *SCOP* due to the undersizing of the borehole field (up to 5% compared to an appropriately sized field with the same solar collector area), as mentioned above, the use of solar collectors could be a key factor to consider and deeper investigate in future works, also in relation to the initial investment cost of the borehole field. Additional investigations may also take into account the influence of different soil properties, or of the convection in the soil [26], and the effect of real weather data on the temperature drift in ground-source heat pumps coupled with solar collectors. Moreover, an economic analysis of substituting the old generation system with the one proposed in this study will also be conducted, also considering the reduction in carbon dioxide emissions.

Author Contributions: Conceptualization, E.R.d.S. and P.V.; methodology, V.B., E.R.d.S., P.V., C.N. and M.D.; software and investigation, V.B. and P.V.; validation, M.D. and C.N.; writing—original draft preparation, V.B., E.R.d.S. and P.V.; writing—review and editing, V.B., E.R.d.S., P.V., C.N. and M.D.; supervision, E.R.d.S. and P.V.; funding acquisition, E.R.d.S. All authors have read and agreed to the published version of the manuscript.

Funding: The research leading to these results has received funding from Italian PNRR—Missione 4—Componente 2, Investimento 1.5 Creazione e rafforzamento di Ecosistemi dell'innovazione, costruzione di leader territoriali di R&S D.D. 3277 del 30 December 2021, under the research project ECOSISTER-Ecosystem for Sustainable Transition in Emilia-Romagna (Spoke N. 2—Clean energy production, storage and saving), Code ECS00000033, CUP J33C22001240001.

Institutional Review Board Statement: Not applicable.

Informed Consent Statement: Not applicable.

Data Availability Statement: Data are available on request.

Conflicts of Interest: The authors declare no conflict of interest.

References

1. European Commission. *Communication from the Commission to the European Parliament, the Council, the European Economic and Social Committee and the Committee of the Regions a Renovation Wave for Europe—Greening our Buildings, Creating Jobs, Improving Lives*; European Commission: Brussels, Belgium, 2020.
2. Valdiserri, P.; Ballerini, V.; di Schio, E.R. Interpolating functions for CO_2 emission factors in dynamic simulations: The special case of a heat pump. *Sustain. Energy Technol. Assess.* **2022**, *53*, 102725. [CrossRef]
3. Valdiserri, P.; Ballerini, V.; di Schio, E.R. Hourly data for evaluating the carbon dioxide emission factor of heat pumps or other devices connected to the Italian grid. *Data Brief* **2022**, *45*, 108682. [CrossRef] [PubMed]
4. European Commission. Renovation and Decarbonisation of Buildings. Available online: https://ec.europa.eu/commission/presscorner/detail/en/IP_21_6683 (accessed on 11 May 2023).
5. Bianco, V.; Marchitto, A.; Scarpa, F.; Tagliafico, L.A. Heat pumps for buildings heating: Energy, environmental, and economic issues. *Energy Environ.* **2018**, *31*, 116–129. [CrossRef]
6. Pereira, J.; Teixeira, H.; Gomes, M.D.G.; Moret Rodrigues, A. Performance of Solar Control Films on Building Glazing: A Literature Review. *Appl. Sci.* **2022**, *12*, 5923. [CrossRef]
7. Tang, S.K. A review on natural ventilation-enabling façade noise control devices for congested high-rise cities. *Appl. Sci.* **2017**, *7*, 175. [CrossRef]
8. Santolini, E.; Pulvirenti, B.; Guidorzi, P.; Bovo, M.; Torreggiani, D.; Tassinari, P. Analysis of the effects of shading screens on the microclimate of greenhouses and glass facade buildings. *Build. Environ.* **2022**, *211*, 108691. [CrossRef]
9. You, T.; Wu, W.; Yang, H.; Liu, J.; Li, X. Hybrid photovoltaic/thermal and ground source heat pump: Review and perspective. *Renew. Sustain. Energy Rev.* **2021**, *151*, 111569. [CrossRef]
10. Arslan, O.; Arslan, A.E.; Boukelia, T.E. Modelling and optimization of domestic thermal energy storage based heat pump system for geothermal district heating. *Energy Build.* **2023**, *282*, 112792. [CrossRef]
11. Jahanbin, A.; Semprini, G.; Impiombato, A.N.; Biserni, C.; Rossi di Schio, E. Effects of the circuit arrangement on the thermal performance of double U-tube ground heat exchangers. *Energies* **2020**, *13*, 3275. [CrossRef]
12. Lucchi, M.; Lorenzini, M.; Valdiserri, P. Energy performance of a ventilation system for a block of apartments with a ground source heat pump as generation system. *J. Phys. Conf. Ser.* **2017**, *796*, 012034. [CrossRef]
13. Rossi di Schio, E.; Ballerini, V.; Dongellini, M.; Valdiserri, P. Defrosting of Air-Source Heat Pumps: Effect of Real Temperature Data on Seasonal Energy Performance for Different Locations in Italy. *Appl. Sci.* **2021**, *11*, 8003. [CrossRef]
14. Miglioli, A.; Aste, N.; Del Pero, C.; Leonforte, F. Photovoltaic-thermal solar-assisted heat pump systems for building applications: Integration and design methods. *Energy Built Environ.* **2023**, *4*, 39–56. [CrossRef]
15. Bae, S.; Chae, S.; Nam, Y. Performance Analysis of Integrated Photovoltaic-Thermal and Air Source Heat Pump System through Energy Simulation. *Energies* **2022**, *15*, 528. [CrossRef]
16. Matera, N.; Mazzeo, D.; Baglivo, C.; Congedo, P.M. Will Climate Change Affect Photovoltaic Performances? A Long-Term Analysis from 1971 to 2100 in Italy. *Energies* **2022**, *15*, 9546. [CrossRef]
17. European Commission. Climate Action Paris Agreement. Available online: https://unfccc.int/process-and-meetings/the-paris-agreement/the-paris-agreement (accessed on 11 May 2023).
18. Guelpa, E.; Verda, V. Thermal energy storage in district heating and cooling systems: A review. *Appl. Energy* **2019**, *252*, 113474. [CrossRef]
19. Ciampi, G.; Rosato, A.; Sibilio, S. Thermo-economic sensitivity analysis by dynamic simulations of a small Italian solar district heating system with a seasonal borehole thermal energy storage. *Energy* **2018**, *143*, 757–771. [CrossRef]
20. Tanaka, H.; Tomita, T.; Okumiya, M. Feasibility study of a district energy system with seasonal water thermal storage. *Sol. Energy* **2000**, *69*, 535–547. [CrossRef]
21. Trillat-Berdal, V.; Souyri, B.; Fraisse, G. Experimental study of a ground-coupled heat pump combined with thermal solar collectors. *Energy Build.* **2006**, *38*, 1477–1484. [CrossRef]
22. Zhou, J.; Cui, Z.; Xu, F.; Zhang, G. Performance Analysis of Solar-Assisted Ground-Coupled Heat Pump Systems with Seasonal Thermal Energy Storage to Supply Domestic Hot Water for Campus Buildings in Southern China. *Sustainability* **2021**, *13*, 8344. [CrossRef]
23. Lund, H.; Østergaard, P.A.; Connolly, D.; Ridjan, I.; Mathiesen, B.V.; Hvelplund, F.; Thellufsen, Z.J.; Sorknaes, P. Energy Storage and Smart Energy Systems. *Int. J. Sustain. Energy Plan. Manag.* **2016**, *11*, 3–14.
24. Klein, S.A.; Duffie, A.J.; Mitchell, J.C.; Kummer, J.P.; Thornton, J.W.; Bradley, D.E.; Arias, D.A.; Beckman, W.A. *TRNSYS 17—A TRaNsient SYstem Simulation Program, User Manual. Multizone Building Modeling with Type 56 and TRNBuild*; Version 17.1; University of Wisconsin: Madison, WI, USA, 2010.
25. Klein, S.A.; Duffie, A.J.; Mitchell, J.C.; Kummer, J.P.; Thornton, J.W.; Bradley, D.E.; Arias, D.A.; Beckman, W.A.; Braun, J.E.; Urban, R.E.; et al. *TRNSYS 17: A Transient System Simulation Program*; University of Wisconsin: Madison, WI, USA, 2010.
26. Rossi Di Schio, E.; Lazzari, S.; Abbati, A. Natural convection effects in the heat transfer from a buried pipeline. *Appl. Therm. Eng.* **2016**, *102*, 227–233. [CrossRef]